Life prediction based on biaxial fatigue crack growth simulated in different microstructures modeled by using Voronoi-polygons

AUTHOR(S):

Hoshide, Toshihiko

Available online at www.sciencedirect.com
ScienceDirect
Procedia Engineering 2 (2010) 111–120
Procedia Engineering
www.elsevier.com/locate/procedia

Fatigue 2010

Life prediction based on biaxial fatigue crack growth simulated in different microstructures modeled by using Voronoi-polygons

Toshihiko Hoshide[a]*

[a]*Department of Energy Conversion Science, Graduate School of Energy Science, Kyoto University, Yoshida-Honmachi, Kyoto 606-8501, Japan*

Received 8 February 2010; revised 10 March 2010; accepted 15 March 2010

Abstract

Fatigue life is significantly affected by the crack growth behavior that depends on the material microstructure as well as the stress biaxiality. By considering such effects of microstructure and stress state on crack growth, a methodology to predict failure life in biaxial fatigue of materials with different microstructures was proposed in the present work. For more appropriate modeling, an aggregate of Voronoi-polygons was adopted to express microstructural features of polycrystalline materials. In the microstructure modeled by an aggregate of Voronoi-polygons, the crack initiation was quantitatively analyzed by considering the slip deformation on slip plane which is randomly set in each Voronoi-polygon. The algorithm for the crack growth was established as a competition between the growth by crack coalescences and the propagation of a dominant crack as a single crack. The coalescence growth under the assumed criteria was also taken into account among initiated and/or propagating cracks during the whole fatigue process. The failure life was statistically predicted based on the crack growth behavior simulated for forty distinct microstructural configurations, which were formed by generating different combinations of randomized shapes of Voronoi-polygons for the same material. By applying the proposed analytical procedure, simulations were conducted according to the same conditions as experimental ones in fatigue tests, which had been carried out under axial, torsional and combined loading modes by using circumferentially-notched specimens of pure copper, medium carbon steel, and (α+β) and β titanium alloys. In this case, forty different failure-lives were obtained for each combination of material and loading mode. It was revealed that the failure lives observed in experiments were almost covered by the life-ranges between the minimum and the maximum lives given in simulation. It was also clarified that a dispersion of simulated lives was found to be larger at higher stress level.

Keywords: Biaxial fatigue; Life prediction; Fatigue crack growth; Modeling; Microstructure; Voronoi-polygon; Monte Carlo simulation; Pure copper; Medium carbon steel; Titanium alloy

1. Introduction

It is well known that cracking behavior, which affects failure life remarkably, depends on the level and the multiaxiality of the applied stress as well as the material microstructure [1, 2]. For more realistic assessments of failure life of machine components subjected to complex stresses, some models of the fatigue process have been proposed to describe the cracking behavior in modeled microstructures under biaxial stress state [3-9]. There is,

* Corresponding author. Tel.:+81-75-753-5862; fax:-81-75-753-5862.
E-mail address: Toshi.Hoshide@ecs.mbox.media.kyoto-u.ac.jp.

1877-7058
doi:10.1016/j.proeng.2010.03.012

however, no simple model adequately to express geometric features of a complex microstructure of polycrystalline material under consideration. Recently, notice has been taken to a Voronoi diagram [10] in modeling a material microstructure. The application of such a modeling is expected in solving the aforementioned problem.

In the present work, a previous analytical procedure [9] is developed so that a modeling of microstructure in polycrystalline material should be improved especially. In modeling a microstructure, an aggregate of Voronoi-polygons is used, and an analytical procedure is developed to be more applicable to biaxial fatigue behavior in notched components of materials with different microstructures. A quasi-three dimensional modeling is newly introduced in the analysis of crack initiation. Using the developed procedure, a computer simulation of Monte Carlo type is made to clarify the statistical characteristics of fatigue life in four kinds of materials with different microstructures under axial, torsional and combined axial-torsional loading modes. The applicability of the developed procedure is investigated by comparing simulated results with experimental observations.

2. Materials and Fatigue Testing Conditions to Be Analyzed

A brief outline of experimental fatigue tests, which will be analyzed by using a proposed procedure, is mentioned in this section.

The materials to be considered in the following analyses are four kinds of materials; an oxygen-free pure copper with purity of 99.98%, a medium carbon steel including 0.45wt% C, and two types of Ti-6Al-4V titanium (Ti) alloys having (α+β) phases and β phase. Mechanical properties of these materials are as follows: yield strength σ_y = 83MPa, elongation φ = 0.80, Young's modulus E = 139GPa and Poisson's ratio ν = 0.37 in pure copper; σ_y = 410MPa, φ = 0.38, E = 206GPa and ν = 0.23 in medium carbon steel; σ_y = 911MPa, φ = 0.19, E = 110GPa and ν = 0.35 in (α+β) Ti alloy; σ_y = 849MPa, φ = 0.068 E = 127GPa and ν = 0.41 in β Ti alloy. Mean grain-size d_o is remarkably dependent on material kind, i.e., 55μm in pure copper, 21μm in medium carbon steel, 8.5μm in (α+β) Ti alloy, and 400μm in β Ti alloy.

Solid cylindrical bars of the four materials were machined to have blunt notches in their circumferential directions. The notch-root radius R was prepared to be two sizes for pure copper and medium carbon steel, i.e., R = 3mm and R = 5 mm, while R = 6mm was selected as the notch-root radius for two Ti alloys. The fatigue life and cracking behavior around notched portions in specimens of the four materials had been investigated experimentally in our other works [5, 6, 11].

Fatigue tests were conducted under fully reversed and force-controlled conditions in axial, combined axial-torsional and torsional modes. Fatigue testing conditions were determined by using the axial stress range $\Delta\sigma_z$ and the shear stress range $\Delta\tau_{z\theta}$. The stress components are specified in a cylindrical orthogonal-coordinate r-θ-z system. In the coordinate system, the axes of θ and z are respectively set in the circumferential and axial directions of a specimen, while the r-axis coincides with the normal direction of specimen surface.

The range of equivalent stress at the notch-root, $\Delta\sigma_{eq}$, is defined based on observed cyclic stress-strain responses as follows; i.e., $\Delta\sigma_{eq} = (\Delta\sigma_z^2 + 4\Delta\tau_{z\theta}^2)^{1/2}$ for pure copper, and $\Delta\sigma_{eq} = (\Delta\sigma_z^2 + 3\Delta\tau_{z\theta}^2)^{1/2}$ for the other materials. As stress levels of $\Delta\sigma_{eq}$, 388MPa and 465MPa in pure copper, 1000MPa and 1200MPa in medium carbon steel, 1800MP, 2000MPa and 2200MPa in (α+β) Ti alloy, and 1700MPa, 1900MPa and 2100MPa in β Ti alloy are respectively adopted. Combined axial-torsional fatigue tests were carried out by setting the ration of $\Delta\tau_{z\theta}/\Delta\sigma_z$ to be 1.5 for pure copper and medium carbon steel, and 1.73 for the two Ti alloys.

3. Analytical Procedure

Analytical procedure, consisting of modeling of material microstructure by using Voronoi-polygons and a competition model for fatigue crack growth under biaxial stresses, is described in the following.

3.1. Modeling of material microstructure by using Voronoi-polygons

It is well known that most of fatigue cracks are initiated on surfaces of stressed elements except for materials in which cracks are initiated from inclusions inside. In this work, the microstructure on the notch-root surface of a specimen is modeled in a two-dimensional area by using Voronoi-polygons. A Voronoi diagram is a kind of decomposition of a metric space, which is determined by distances to a specified discrete set of points in the space

[10]. It is also known that an aggregate of convex hexagons is easily obtained as Voronoi-polygons in a two-dimensional Voronoi diagram. The merit in adopting Voronoi-polygons as modeling of a microstructure of polycrystalline material is that a microstructural modeling is easily possible by a simple algorithm in conducting numerical analysis.

The size of the aforementioned two-dimensional area is determined as follows. In the case treating notched specimens, it should be noted that the stresses in the region around notch-root decrease when moving away from the notch-root in the axial direction. Such a stress gradient and its effects on crack initiation and propagation should be taken into account in the crack growth analysis. For convenience, in this work, the area to be analyzed in this simulation is restricted in the axial direction so that an axial or shear stress generated on the surface of the notch area must exceed at least 95% of the maximum stress at the notch-root. Finally, sizes in the circumferential (θ) direction and in the axial (z) direction are set depending on material and notch geometry. In the analyzed area, the number of Voronoi-polygons, n, is determined so that the resultant mean grain-size should approximately equals to the size measured in experiment. The determination of polygon-number is the final process for a material consisting of one phase, such as pure copper or β Ti alloy.

On the other hand, medium carbon steel consists of ferrite and pearlite grains, and (α+β) Ti alloy has α- and β-phase grains in their microstructures. For these materials, Voronoi-polygons are randomly selected among all Voronoi-polygons so that an area-ratio of selected polygons occupying in the analyzed area could coincide with the microstructural composition observed in a material under consideration. In medium carbon steel, by setting the area-ratio to be 0.27, which is experimentally observed in medium carbon steel, the resultantly selected polygons are regarded as pearlite grains. In (α+β) Ti alloy, grains of β-phase are observed to be larger than those of α-phase. Therefore, as for (α+β) Ti alloy, Voronoi-polygons are randomly selected, and each selected Voronoi-polygon is treated as the polygon that nucleates β-phase. Then, the neighboring two Voronoi-polygons for respectively selected polygon nucleating β-phase are clustered into one polygon. The clustered polygon is regarded as a final β-phase grain. This process is iterated so that the area-ratio of β-phase grains occupying in the analyzed area should be 0.42, which is experimentally observed in (α+β) Ti alloy.

Polygons formed as mentioned above are hereafter called grains, which constitutes a polycrystalline material. Figure 1 shows an example of modeled microstructure.

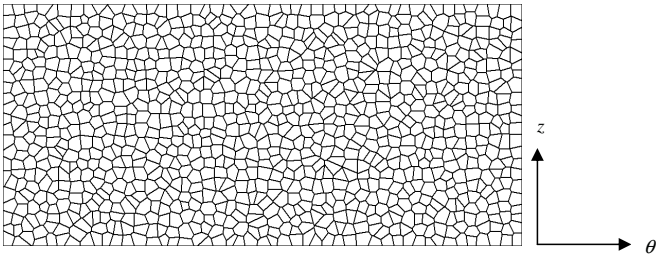

Fig. 1. Example of microstructure modeled by using Voronoi-polygons (pure cooper specimen with notch-root radius R = 5mm)

3.2. Stress state in modeled grain and definition of grain-size

Since individual grains have differences in geometrical shape and deformation response in an actual polycrystalline material, a stress state in one grain is supposed to differ from that in another grain. Therefore, it is reasonable to consider that stresses, to which individual grains are subjected, are different from the applied bulk stress. The present model assumes that stress states in individual grains deviate from the given applied stress state in the crack initiation analysis as follows.

$$\Delta\sigma_z^{(i)} = \Delta\sigma_z f_i,\ \Delta\sigma_\theta^{(i)} = \Delta\sigma_\theta g_i,\ \text{and}\ \Delta\tau_{z\theta}^{(i)} = \Delta\tau_{z\theta} h_i \tag{1}$$

In Eq. (1), $\Delta\sigma_z$, $\Delta\sigma_\theta$ and $\Delta\tau_{z\theta}$ are respectively axial, hoop and shear stress range components of the applied bulk stress, and $\Delta\sigma_z^{(i)}$, $\Delta\sigma_\theta^{(i)}$ and $\Delta\tau_{z\theta}^{(i)}$ are the stress range components in the i-th grain. These stress ranges are defined in the aforementioned r-θ-z coordinate system. Deviation factors f_i, g_i and h_i in Eq. (1) are randomly given within the range from 0.5 to 1.5 so that they should satisfy the condition specified in Eq. (2).

$$\sum_{i=1}^{n} f_i/n = 1,\ \sum_{i=1}^{n} g_i/n = 1,\ \text{and}\ \sum_{i=1}^{n} h_i/n = 1 \tag{2}$$

In Eq. (2), n is the aforementioned number of grains set in the analyzed area.

The grain-size d is defined as the length of line-segment passing through the nucleus-point in a Voronoi-polygon as illustrated in Fig. 2. In the following analysis of crack initiation, the grain-size $d^{(i)}$ of the i-th grain will be also used as the slip-band length in the grain.

3.3. Competition model for fatigue crack growth under biaxial stresses

A competition model for crack growth established in our works [3, 4, 6, 9] is also applied in the present simulation. The model postulates that the cracking morphology and the fatigue failure life are determined as the result of competition between the growth by crack coalescence and the propagation of a main crack as a single crack. The competition implies that the dominant crack growth will be governed by the faster growth mode. Each analytical procedure is summarized in the following.

3.3.1. Crack initiation analysis

In the crack initiation analysis too, the r-θ-z coordinate system is employed as depicted in Fig. 2. The z-axis is set to be parallel to the axial direction of specimen. Consider a slip plane in one grain on the specimen surface. On the slip plane, another orthogonal ξ–η–ζ coordinate is also introduced so that the ξ- and η- axes should be respectively parallel to the normal direction of the slip plane and the slip direction on the slip plane.

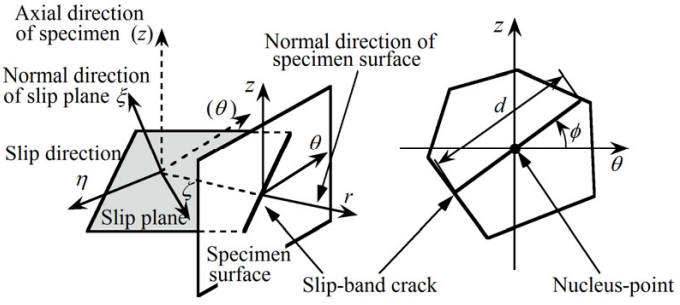

Fig. 2. Geometric relation of slip plane to specimen surface, and direction of slip-band crack

Table 1. Directional cosines between r–θ–z and ξ–η–ζ axes

Axes	ξ	η	ζ
r	$l_{r\xi}$	$l_{r\eta}$	$l_{r\zeta}$
θ	$l_{\theta\xi}$	$l_{\theta\eta}$	$l_{\theta\zeta}$
z	$l_{z\xi}$	$l_{z\eta}$	$l_{z\zeta}$

The directional cosine tensor [l] is used for the transformation between r-θ–z and ξ–η–ζ coordinates. For the coordinates, the components of [l] are defined as shown in Table 1.

By using the directional cosine tensor [l], the stress component [$\sigma_{\xi\eta\zeta}$] for the slip system is correlated with an applied stress [$\sigma_{r\theta z}$] as Eq. (3).

$$[\sigma_{\xi\eta\zeta}] = [l]\,[\sigma_{r\theta z}]\,[l]^{\mathrm{T}} \tag{3}$$

In Eq. (3), the superscript "T" represents the transposed matrix,

$$[\sigma_{r\theta z}] = \begin{vmatrix} \sigma_r & \tau_{r\theta} & \tau_{rz} \\ \tau_{\theta r} & \sigma_\theta & \tau_{\theta z} \\ \tau_{zr} & \tau_{z\theta} & \sigma_z \end{vmatrix}, \text{ and } [\sigma_{\xi\eta\zeta}] = \begin{vmatrix} \sigma_\xi & \tau_{\xi\eta} & \tau_{\xi\zeta} \\ \tau_{\eta\xi} & \sigma_\eta & \tau_{\eta\zeta} \\ \tau_{\zeta\xi} & \tau_{\zeta\eta} & \sigma_\zeta \end{vmatrix}$$

Considering slip in a surface grain, we may assume the plane stress state as $\sigma_r = \tau_{rz} = \tau_{zr} = \tau_{r\theta} = \tau_{\theta r} = 0$. Under the above assumption, the resolved shear stress $\tau_{\xi\eta}$ in the slip direction on the associated slip plane, which is one of the most important factors for the feasibility to slip, is represented by

$$\tau_{\xi\eta} = \sigma_z\, l_{z\eta}\, l_{\theta\eta} + \sigma_\theta\, l_{z\xi}\, l_{\theta\xi} + \tau_{z\theta}\,(l_{z\xi}\, l_{\theta\eta} + l_{z\eta}\, l_{\theta\xi}) \tag{4}$$

As illustrated in Fig. 2, the angle ϕ of a slip-band is defined counterclockwise against the θ–axis on the specimen surface, and is calculated as follows.

$$\phi = \arctan\,(-l_{\theta\xi} / l_{z\xi}) \tag{5}$$

In this model, a crack is assumed to be initiated along the slip band when the criterion, $\tau_{\xi\eta} \geq \tau_c$ in which τ_c is the critical shear stress to make a slip active, is satisfied, and also the number of stress cycles exceeds the cycle number N_i, which is required to make a slip band into a crack. The parameter N_i is identical to the crack initiation life, and is calculated by using a dislocation pile-up model [12] as

$$N_i = \frac{2\,G\,W_c}{\pi\,(1-\nu)\,d\,(\tau_{\xi\eta} - \tau_c)^2} \tag{6}$$

In Eq. (6), material constants G, ν and W_c are respectively the shear elastic modulus, Poisson's ratio and the surface energy, all of which are material constants. The parameter d is the length of slip band, though d may change depending on a grain to be considered in the slip analysis. Note that the crack initiation life in a certain grain is different from those in other grains, even if the modeled configuration of microstructure is identical and the same stress state is applied. This means that the initiation of cracks in an analyzed area can be observed at arbitrary position and at arbitrary number of stress cycles.

3.3.2. Crack propagation analysis

The mode of crack propagation is analyzed presuming that the growth rate da/dN is expressed by a power function of the J-integral range, ΔJ, as follows.

$$\frac{\mathrm{d}a}{\mathrm{d}N} = C\,\Delta J^{m} \tag{7}$$

In Eq. (7), C and m are material constants. J-integral range is evaluated assuming that short suface-cracks are semi-circluar. The evaluation of J-integral range for short surface-cracks is given elsewhere [13, 14]. The propagation life required for a given crack extension can be calculated by integrating Eq. (7) with respect to the

crack length. The integral calculation is also employed in determining the time at which a subsequent crack linkage occurs, or the failure life which is defined by a given crack length.

3.3.3. Crack coalescence analyses

During the crack initiation and propagation stages, the coalescence growth is taken into account among distributed cracks, or propagating cracks. In the crack initiation stage, a newly initiated crack is assumed to link with one of previously initiated cracks, if the tip-to-tip distance between the cracks (see Fig. 3) is less than a specific length $\xi\, d_o$. The size d_o is the mean grain-size for the modeled microstructure. The coalescence in the crack propagation stage is presumed to occur when the tip-to-tip distance between the main and the secondary cracks (see Fig. 4) becomes less than $\zeta\, d_o$. The values of ξ and ζ, which depend on the combination of material microstructure and loading mode, are determined according to experimental observations. Larger value of ξ or ζ implies that cracks can more easily coalesce together. When one of tips of a crack reaches a boundary of the analyzed area, the growth analysis for the crack is discontinued.

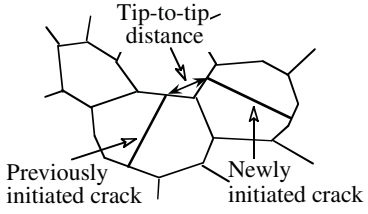

Fig. 3. Coalescence analysis in initiation stage

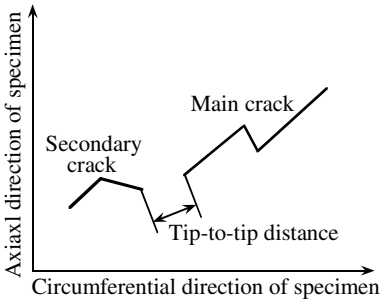

Fig.4 . Coalescence analysis in propagation stage

4. Simulated Results and Discussion

4.1. Simulation procedure

Values of parameters used in the simulation are determined for each material and respective loading mode. However, it is difficult to estimate the coalescence parameters ξ and ζ for lack of experimental observations concerning more various materials and loading modes. Therefore, the parameters ξ and ζ have been determined according to the observation of actual crack coalescence behavior in experiment [15].

Numerical simulations for the fatigue testing conditions as mentioned previously are executed by using a Monte Carlo type procedure. Employing forty series of uniform random numbers, forty distinct modeled microstructures are generated for a material to be analyzed. Such forty microstructures are respectively composed of differently-shaped grains and have distinct combinations of directions of slip-lines and slip-planes in the individual grains. The crack growth under each condition of fatigue testing is analyzed in respective modeled microstructure of the material. Forty distinct cracking patterns can be finally obtained for each material under a given condition of fatigue testing through Monte Carlo simulations.

4.2. Comparison of simulated results with experimental ones

Figure 5 presents examples of cracking morphology simulated for (α+β) Ti alloy. In Fig. 5, a dominant crack and sub-cracks are depicted with bold and thin lines, respectively. Unfortunately, the feature is not clear in axial loading mode. It is seen, however, that the dominant crack grows in the direction perpendicular to the direction of the

maximum principal stress under combined loading. On the other hand, the torsional mode brings about the main crack in the axial direction which coincides with the direction of the maximum shear stress. Such features and the dependence on the stress state of cracking morphology, which had been observed experimentally [5, 6, 10], are adequately simulated by using the proposed procedure.

By monitoring cracking behavior during a simulation, a crack growth curve is given as the relation between the number of cycles N and the length a of main crack for a material subjected to a prescribed loading mode. Such a crack growth curve enables us to determine the failure life defined by a specified crack length. Since forty trials are carried out in the simulation as mentioned previously, forty different crack growth curves are obtained. Figure 6 shows a schematic illustration on the relation between crack growth curves and failure life.

The failure life N_f in experiments is defined as the number of cycles, at which a dominant crack of a specified length a_c is formed at the notched portion. In simulations, as shown in Fig. 6, the failure life is calculated as the formation cycles leading to the dominant crack with a specified length a_c for consistency with the experiment of each material. The crack length is specified according to experimental observations [5, 6, 11]. The specified crack lengths to be adopted in the present analysis are respectively 2mm for pure copper, 1mm for medium carbon steel, 0.3mm for (α+β) Ti alloy, and 3mm for β Ti alloy.

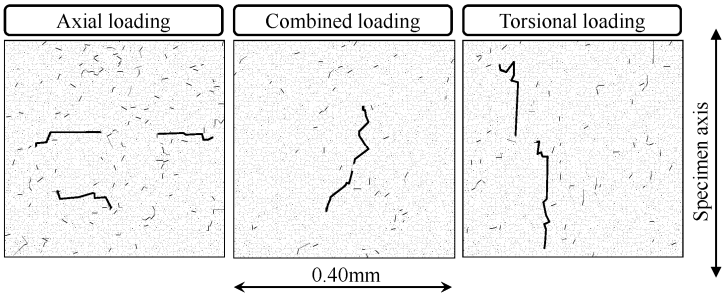

Fig. 5. Examples of simulated cracking morphology in (α+β) Ti alloy specimen with notch-root radius R = 6mm

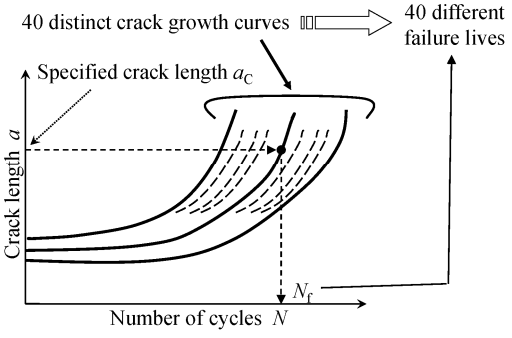

Fig. 6. Schematic illustration of crack growth curve

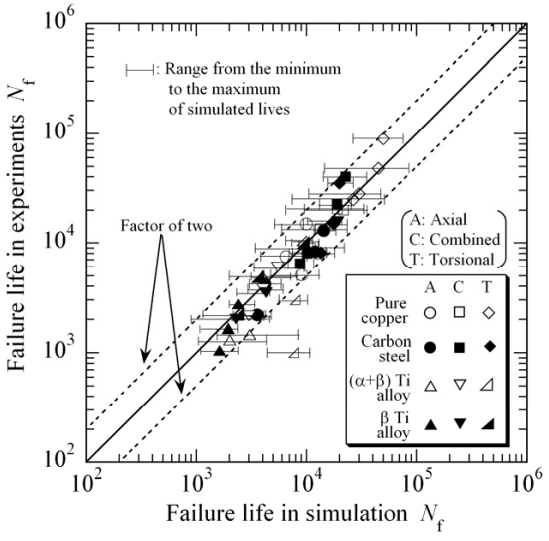

Fig. 7. Comparison between simulated and experimental failure life

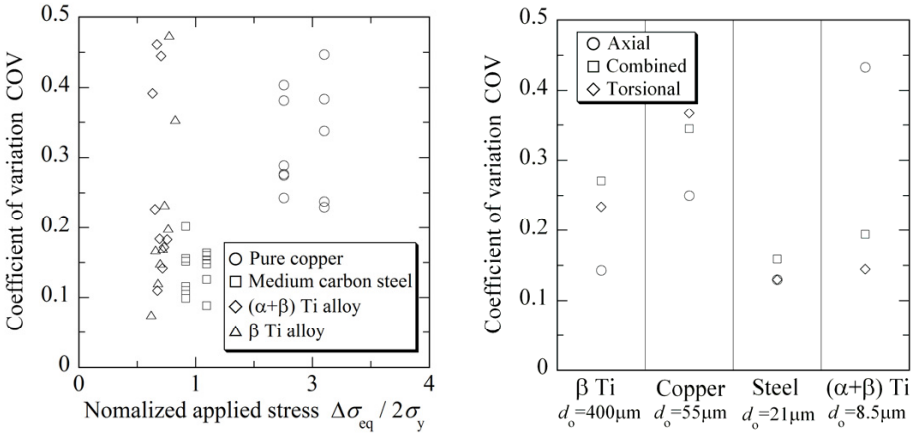

(a) Correlation with normalized stress level. (b) Dependence on material kind.

Fig. 8. Coefficient of variation of simulated lives.

Figure 7 shows the comparison between the actual failure life observed in experiments and the simulated life. In the figure, each symbol presents a data point of the actual life correlated with the average life of forty lives simulated for the corresponding material under one testing condition, and the life-range from the minimum and the maximum lives is drawn with an error-bar. Two dotted-straight lines in Fig. 7 represent factors of two in the life

dispersion. It is found that the predicted life-ranges almost cover actual failure lives in experiments, though the data simulated for (α+β) Ti alloy under torsional loading appear to shift toward longer life region beyond the factor of two. Considering a possible scatter of failure life to appear in experiments, however, it may be generally concluded that the proposed procedure gives a good estimation for the failure life in materials with various microstructures under biaxial fatigue.

The failure life obtained by simulation has large scatter as seen in Fig. 7. Such a scatter is discussed by using the coefficient of variation of simulated lives. For each testing condition in a respective material, the coefficient of variation is defined as the standard deviation of lives divided by the average life. Figure 8(a) presents the coefficient of variation correlated with the equivalent stress range $\Delta\sigma_{eq}$ normalized by the twice the value of yield stress σ_y. As a whole trend, the coefficient of variation increases with increasing the level of applied stress. This implies that a scatter of simulated life becomes larger as the level of applied stress is increased. Such a trend may be explained as follows. Consider the case of lower stress level at first. In this case, the number of initiated cracks is smaller, and so the crack growth unaccompanied by crack coalescence is expected. Many cracks, however, are expected to be initiated at higher stress level. In such a situation as many cracks exist, the crack coalescence mode affects the life variation. When crack coalescences occur oftener during fatigue process, a crack grows earlier at smaller number of cycles; i.e., the failure life is decreased because the failure life is specified by the crack length. When crack coalescences hardly occur during fatigue process, the number of cycles required for a crack length reaching a specified one becomes larger. Consequently, it is suggested that the variation of failure life may be larger with increasing the stress level. It is also seen in Fig. 8(a) that the inclinations in the relations between the coefficient of variation and the applied stress level in the two Ti alloys is steeper than those in pure copper and medium carbon steel. It seems obvious that the life scatter in the Ti alloys is more sensitive to the stress level compared with those of the other materials. On the other hand, the dependence of life scatter on material kind is depicted in Fig. 8(b), where the averaged value of coefficient of variation is plotted for the same loading mode. In single-phase materials, i.e., β Ti alloy and pure copper, the life dispersion under axial loading mode is smaller than those under the other two modes, while the difference in the dispersion is not so large between the combined and torsional modes. As for dual-phase materials, i.e., medium carbon steel and (α+β) Ti alloy, large dependence on loading mode is not seen in medium carbon steel, but the life dispersion under axial loading mode is much larger than those under the other modes in (α+β) Ti alloy. In both types of materials having single- or dual-phases, the life scatter is found to be larger in materials with finer grains. This is ascribed to the dominance of propagation as a single crack in coarser grained material, in which larger cracks are initiated.

5. Summary

Fatigue life is affected by the crack growth behavior which depends on the material microstructure as well as the stress biaxiality. For more realistic assessments of failure life of machine components subjected to complex stresses, some models of the fatigue process are required to describe such a cracking behavior in biaxial stress state as well as feature of material microstructure.

In the present work, a model of fatigue crack growth under biaxial stresses was developed to simulate cracking behavior and to evaluate failure life for notched components. In modeling, especially, an aggregate of Voronoi-polygons was adopted to express microstructural features of a polycrystalline material adequately. An algorithm for the crack growth in the microstructure modeled by using Voronoi-polygons was established by applying a competition model. The competition model postulated that the cracking behavior and the failure life were determined as a result of competition between the growth by crack coalescence, and the propagation of a main crack as a single crack. It was also assumed that a crack was initiated along the slip band when the resolved shear stress became larger than the critical shear stress to make a slip active, and also when the number of stress cycles exceeded the cycle number which was necessary for making a slip band into a crack. The mode of crack propagation was analyzed in terms of the relation of crack growth rate correlated with *J*-integral range. The propagation life required for a given crack extension was calculated by integrating the crack propagation law with respect to the crack length. During the crack initiation and propagation stages, a coalescence growth under the assumed criteria was taken into account among distributed cracks, or propagating cracks.

The applicability of the proposed procedure was discussed by executing Monte Carlo type simulations for fatigue testing conditions in experiments. For each testing condition, forty distinct microstructural configurations were

generated by using forty different combinations of Voronoi-polygons randomized in their shapes. The failure life was defined as the number of cycles required for the formation of crack with a specified length, and the life was statistically estimated by simulated crack growth curves. In such simulations, forty different failure lives were obtained by the prediction based on the crack growth analysis for respective microstructure. Simulated results were compared with experimental observations in previous fatigue tests of circumferentially notched specimens, which had been conducted using pure copper, medium carbon steel, and (α+β) and β Ti alloys under axial, combined axial-torsional and torsional loading. The features in actually observed cracking patterns, depending on the combination of material microstructure and loading mode, were almost represented by simulated cracking morphologies. It was clarified that the failure life was appropriately simulated excepting a few cases. Considering life scatter to be expected in experiments, it may be concluded that the failure life was adequately predicted by using the proposed procedure. The variation of simulated failure life was found to become larger with increasing the applied stress level. It was laso suggested that the life variation in the two Ti alloys was more sensitive to the stress level compared with those in pure copper and medium carbon steel.

Acknowledgements

The author wishes to thank Mr. Sata, Mr. Takahashi, Mr. Kasai and Mr. Adachi, who were previous students of Kyoto University, for their cooperation to this work.

References

[1] Hua CT, Socie DF. Fatigue damage in 1045 steel under variable amplitude biaxial loading. *Fatigue Fract Eng Mater Struct* 1985; **8**: p. 101–114.
[2] Bannatine JA, Socie DF. Observations of cracking behavior in tension and torsion low cycle fatigue. *ASTM STP 942*; 1988: p. 899–921.
[3] Hoshide T. Socie DF. Crack nucleation and growth modeling in Biaxial fatigue. *Eng Fract Mech* 1988; **29**: 287–299.
[4] Hoshide T, Kawabata T, Inoue T. Analysis of intergranular cracking in low cycle fatigue under biaxial stresses. *Trans Jpn Soc Mech Engnr*, Ser. A 1989; **55**: 222–230.
[5] Hoshide T, Yokota K, Inoue T. Investigation on small crack growth and life predictions in fatigue of circumferentially-notched component of pure copper subjected to combined loading. *J Soc Mater Sci, Jpn* 1990; **39**: 144–149.
[6] Hoshide T, Inoue T. A modeling of cracking behavior in multiaxial loading. In: Kitagawa H, Tanaka T. editors. *Proc 4th Int Conf Fatigue and Fatigue Thresholds, Fatigue '90* 1990; **IV**: p.2161–2166.
[7] Argence T, Weiss J, Pineau A. Observation and modelling of transgranular and intergranular multiaxial low-cycle fatigue damage of austenitic stainless steel. In: Pineau A, Cailetaud G, Lindley TC. editors. *Multiaxial Fatigue and Design,* Mechanical Engineering Publications, UK 1996: p. 209–227.
[8] Socie DF, Furman S. Fatigue damage simulation models for multiaxial loading. In: G. Lütjering G, Nowack H. editors. *Proc. 6th Int. Conf. Fatigue Congress, Fatigue '96* 1996; **II**: p. 967–976.
[9] Hoshide T, Kusuura T. Life prediction by simulation of crack growth in notched components with different microstructures and under multiaxial fatigue. *Fatigue Fract Eng Mater Struct* 1998; **21**: 201–213.
[10] Okabe A, Boots B, Sugihara K, Chiu SN. *Spatial tessellations - concepts and applications of Voronoi diagrams*. 2nd ed. Chichester: John Wiley; 2000.
[11] Hoshide T, Hirota T, Inoue T. Fatigue behavior in notched component of (α+β) and β titanium alloys under combined axial-torsional loading. *Mater Sci Res Int* 1995; **1**: 169–174.
[12] Tanaka K, Mura T. A dislocation model for fatigue crack initiation. *Trans ASME J Appl Mech* 1981; **48**: 97–103.
[13] Hoshide T, Yamada T, Fujimura S, Hayashi T. Short crack growth and life prediction in low-cycle fatigue of smooth specimens. *Eng Fract Mech* 1985; **21**: 85–101.
[14] Hoshide T, Socie DF. Mechanics of mixed mode small fatigue crack growth. *Eng Fract Mech* 1987; **26**: 841–850.
[15] Hoshide T, Miyahara M, Inoue T. Life prediction based on analysis of crack coalescence in low cycle fatigue. *Eng Fract Mech* 1987; **27**: 91–101.